Reprinted from

MATERIALS SCIENCE & ENGINEERING A

Materials Science and Engineering A226–228 (1997) 124–128

In-situ observation of cellular growth under rapid solidification conditions

A. Ludwig *, R. Schadt, P.R. Sahm

Gießerei-Institut der RWTH Aachen, 52056 Aachen, Germany

ELSEVIER

ELSEVIER

Materials Science and Engineering A226–228 (1997) 124–128

MATERIALS SCIENCE & ENGINEERING A

In-situ observation of cellular growth under rapid solidification conditions

A. Ludwig *, R. Schadt, P.R. Sahm

Gießerei-Institut der RWTH Aachen, 52056 Aachen, Germany

Abstract

Dynamic studies on the rapid solidification of binary CBr_4–C_2Cl_6 alloys at different hypoeutectic compositions were performed. The samples were solidified in fine glass tubes with a square cross-section by pulling the tube rapidly from a hot into a cold zone. Applying pulling velocities up to 30 mm s^{-1}, local solidification velocities from 0.3 to 2 mm s^{-1} depending on the cooling temperature were achieved. Independent of concentration and solidification velocity, the observed interface morphologies revealed either a cylindrical or elongated cellular pattern, which are often separated by a boundary in pulling direction. The occurrence of these morphologies was found to change instantaneously. The spacings of the cylindrical and the elongated cells were measured as a function of concentration and solidification velocity. The results are discussed with respect to a recent theory for cellular growth. © 1997 Elsevier Science S.A.

Keywords: Cellular growth; Interface morphologies; Rapid solidification

1. Introduction

In directional solidification of alloys, arrays of cells or dendrites are often produced. The cells or dendrites grow with an average spacing and a tip undercooling which are determined by the alloy composition and the imposed growth conditions (velocity and temperature gradient) [1]. For a small range of growth conditions near the breakdown of a planar front, elongated (two-dimensional plate-like) cells are sometimes found [2–7][1]. Further away from the breakdown condition, cylindrical (three-dimensional finger-like) cells are produced [8,9]. Even further away from the planar front stability dendrites are formed.

The array growth of cells with their typical interaction at the tip region has often been treated by oversimplified analytical models [10–12]. Recently, Hunt and coworkers developed a numerical model of cellular and dendritic growth which can predict cellular and dendritic spacings, undercoolings and the transition between those structures [13–15]. They found that stable cellular growth can exist between the so-called array stability limit and the upper stability limit. They fitted their numerical results by non-dimensional analytic expressions [15], for easy comparison with experimental findings.

In this article, experimental studies of the cellular growth of binary CBr_4–C_2Cl_6 alloys at different hypoeutectic compositions at relative high solidification velocities are presented. The appearance of arrays of elongated and cylindrical cells and of morphological changes between those is reported and discussed. The measured spacings are compared with the analytic expression of Hunt and Lu [15].

2. Experimental procedure

In situ observations of the interface morphologies in the CBr_4–C_2Cl_6 system were performed by rapidly pulling long, fine capillary tubes from a furnace into a liquid coolant. The capillaries used in this work had an inner cross-section of 200 × 200 μm^2 with a wall thickness of 100 μm. They were 900 mm long and made of borosilicate glass. They were filled with alloys of different hypoeutectic compositions.

* Corresponding author. E-mail: ludwig@gi.rwth-aachen.de.

[1] A list of references which consider the occurrence of elongated cells can be found in [6].

PII S0921-5093(96)10604-3

The apparatus used in the experiments consisted of a long furnace, a cooling chamber through which the liquid coolant was pumped, and a pulling device, which permitted pulling velocities between 1 and 30 mm s^{-1} to be achieved. For a solidification experiment, the capillary tube was first threaded through the seals of the cooling system. After the walls of the tube were aligned parallel/perpendicular to the optical axis of the microscope, the tube was moved with a constant velocity from the furnace into the coolant. Further details on the experimental procedure and the filling are given in Ref. [7].

The solidification front was observed through the coolant, perpendicularly to the solid–liquid interface and, simultaneously, from the side with an optical microscope. The actual growth rate was obtained from the angle α between the interface normal and the pulling direction by $V = V_0 \cos \alpha$, where V_0 is the pulling velocity. Local solidification velocities V (normal to the solid–liquid interface) between 0.3 and almost 2 mm s^{-1} were achieved.

To obtain an average of α, about five images in chronological order were evaluated. Measuring errors were minimised by measuring and averaging the angles of the two opposite interfaces. The standard deviation of the main average calculated from the angles of the different images was taken as the measuring error for α. Because V_0 could be adjusted quite precisely, the relative measuring error for V was assumed to be equal to the relative error of α. Thus, V could be estimated with an accuracy of about 6%.

The purification of CBr_4 was performed by sublimation. While the recipient was cooled in a dry ice box, the material was sublimated without heating the original flask. A pressure of about $P = 10^{-2}$ mbar was applied. This procedure was repeated seven times. The purity was found not to increase with further sublimation. Alloying was performed by sublimating a defined quantity of C_2Cl_6 to the purified CBr_4. The alloy was again sublimated and molten subsequently to ensure a well defined mixing.

The concentration of the various alloys, C_0, was estimated by measuring the liquidus temperature, T_L, and applying the phase diagram of CBr_4–C_2Cl_6 measured by Mergy et al. [16]. T_L was measured by investigating the melting process under the microscope. In order to achieve homogeneous temperature distribution, a heated water jacket was placed around a 90 mm long section of the tube. The temperature in the centre of the cooling jacket was measured with a resistance thermometer. The thermometer had a relative accuracy of ± 30 mK and the temperature measured within the jacket varied by some ± 20 mK. Thus, the relative accuracy of the entire system was estimated to be about ± 50 mK. Although the temperature distribution within the jacket was found to be quite uniform, T_L varied slightly over a segment length of about 50 mm, indicating small concentration variation (see Table 1).

The spacings of the cylindrical cells were measured by counting the number of cells in a defined area and calculating the equivalent average radius [8]. The spacings of the elongated cells were estimated by drawing a line perpendicular to the lamella and counting the number of intersections. Again an average value was calculated by evaluating five images in chronological order. A measuring error of 5% was found for λ. The spacings of the elongated cells appear to be always smaller than the corresponding spacings of the cylindrical cells by about 5%.

3. Results and discussion

At high pulling velocities, the liquid pool was very long and the solidification front was nearly parallel to the side walls. The first solid was formed in direct contact with the tube walls as surface dendrites which grew mainly in the edges of the tube. After a thin layer of only a few μm thickness covered the tube from inside, the solid–liquid interface revealed a pyramidal geometry. With the exception of the beginning and the end of the solidification region, the solid–liquid interface was macroscopically flat and therefore the growth velocity was constant over most of the half-width of the capillary. The diffusion boundary layers from opposite side planes did not overlap, except in the region where almost the whole liquid was solidified [7].

Fig. 1 shows two morphologies which are typical of the experiments performed: cylindrical cells (Fig. 1(a)) and elongated (lamellar) cells (Fig. 1(b)). They appeared both within the same solidification experiment, independently of concentrations and solidification velocities used. Similar to the elongated cellular pattern, the cylindrical cellular pattern may reveal an alignment of the cells so that certain directions are preferred (Fig. 1(a)). On the other hand, elongated cells may have a light periodical structure perpendicular to the lamella,

Table 1
Estimated liquidus temperatures, T_L, and the related concentrations, C_0, with the corresponding measuring errors. C_0 was determined using the phase diagram of Mergy et al. [16]

T_L (°C)	Error (°C)	C_0 (wt.%)	Error (wt.%)
93.45	±0.08	Pure[a]	—
91.35	±0.10	1.35	±0.12
89.35	±0.15	3.61	±0.17
88.70	±0.30	4.32	±0.32
87.05	±0.16	6.06	±0.17
85.70	±0.18	7.46	±0.18

[a] A solid-line interval caused by unknown impurities of $\Delta T_0 \cong 0.3$ K was measured for the purified CBr_4.

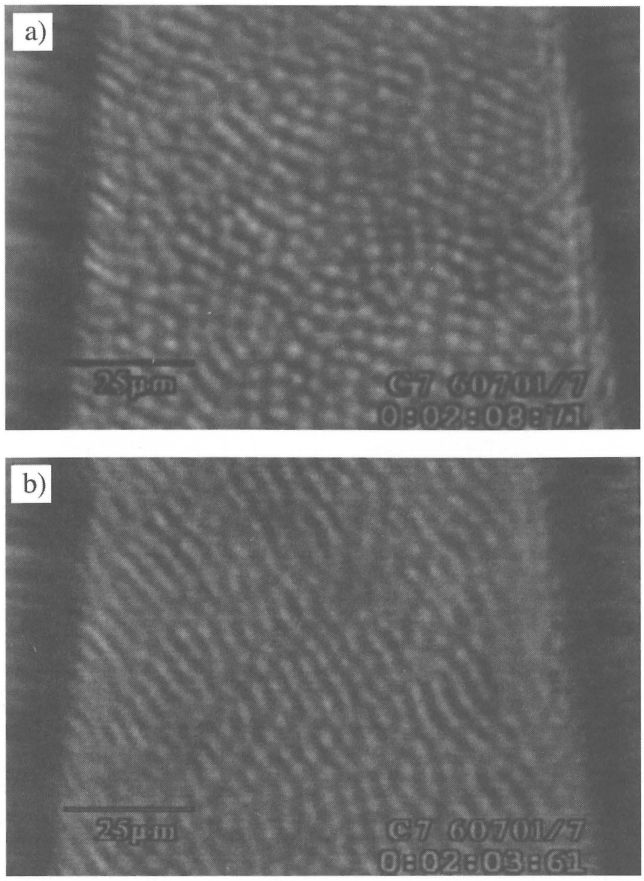

Fig. 1. The observed cellular interface morphologies revealed either a cylindrical (a) or elongated (b) cellular pattern. Morphologies taken from a CBr_4–C_2Cl_6 alloy with a measured liquidus temperature of $T_L = 88.70°C$ solidified with a solidification velocity of $V = 0.5$ mm s^{-1} are shown. The pulling velocity was $V_0 = 5.3$ mm s^{-1}.

which shows that they are about to become cylindrical (Fig. 1(b)).

Cylindrical and elongated cells can either occur separately (as shown in Fig. 1) or at the same time within two (rarely three) different domains. These domains are separated by a boundary which often revealed a small inclination of some degree with respect to the pulling direction (Fig. 2(a)) or even show a sharp turn from normal to perpendicular to the pulling direction (Fig. 2(b)). During the same experimental run, the morphology often changed from only cylindrical cells to only elongated cells and to both patterns separated by the boundary. The latter morphology was most common, whereas elongated cells only were relatively rare.

The rapid change in the morphologies on both sides of the boundary is shown in Fig. 3(a) and (b). First the elongated cells are on the left hand side of the boundary and the cylindrical cells on the right. Within a time period of $\Delta t = 100$ ms, the situation is reversed.

Elongated cells were first observed in 1955 by Walton et al. [2] and Tiller and Rutter [3]. They stated that the instability of a planar front occurred by forming a pox-like structure as a stage of development prior to cell formation. The cells first appeared to be irregular and elongated. Closer to the cellular region, the elongated cells subdivided to form smaller, almost regular, cells.

The effect of crystal orientation on the initial non-planar interface morphology was investigated by Morris and Winegard in more detail [4]. They found that when the growth direction was near a [100] or [111], the initial breakdown structure consisted of nodes (which also transfer to elongated cells prior to forming regular ones). Near [110], the initial breakdown structure consisted of elongated cells. Recently Ludwig and Kurz showed that the intermediate state of elongated cells occurs not only for the transition from a planar to a cellular morphology at low velocity but also at the limit of absolute stability [6,7].

Extrapolation of these results to our experiments shows that the boundary separating elongated and cylindrical cellular pattern has to be regarded as a grain boundary. Comparison of our results with the predic-

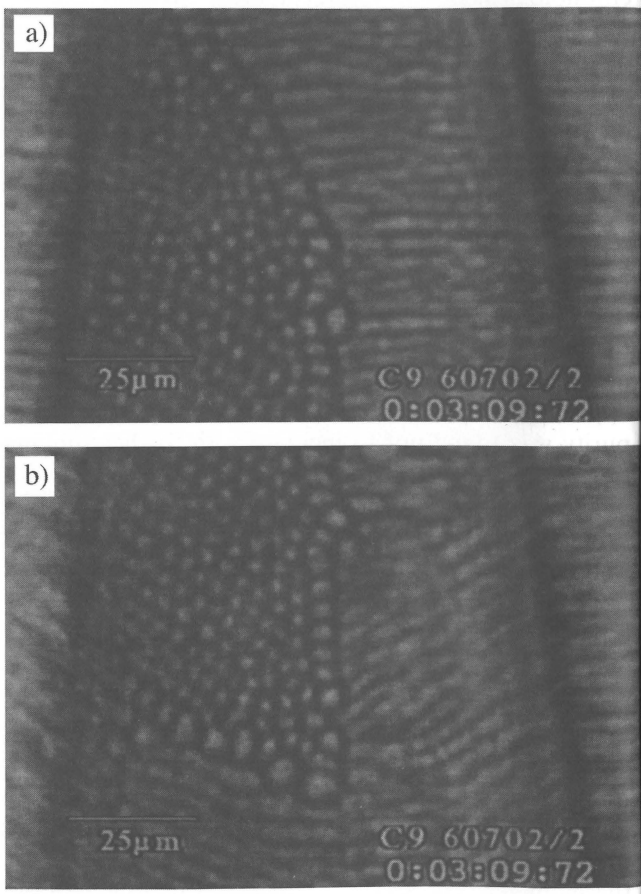

Fig. 2. The boundary separating cylindrical and elongated cellular pattern can reveal an inclination with respect to the pulling direction (a) or even show a sharp turn (b). The liquidus temperature of the alloy shown was measured to be $T_L = 87.05°C$. It solidified with $V = 0.81$ mm s^{-1} and $V_0 = 6.5$ mm s^{-1}. The time difference between (a) and (b) was $\Delta t = 20$ ms.

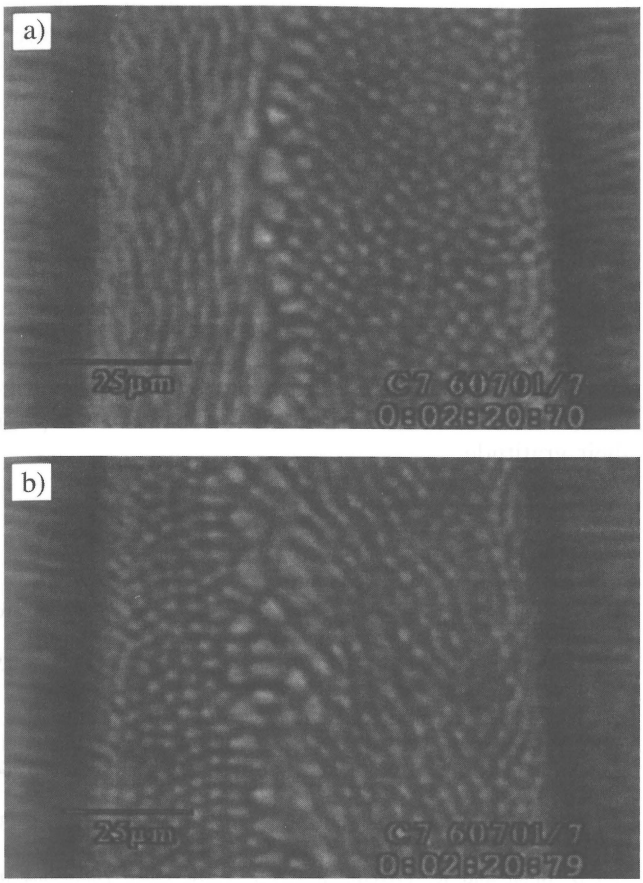

Fig. 3. The morphologies on both sides of the boundary can change very rapidly. Morphologies taken from a CBr_4–C_2Cl_6 alloy with a measured liquidus temperature of $T_L = 88.70$°C solidified with $V = 0.66$ mm s^{-1} and $V_0 = 8.4$ mm s^{-1} are shown: (a) and (b) are taken from the same experimental run with a time difference of $\Delta t = 100$ ms.

tion of Hunt and Lu [15] (see below) reveals that due to the high thermal gradient, the observed cellular pattern grew near the Mullins and Sekerka stability limit V_{MS} [17]. Hence, if both morphologies are observed simultaneously (as in Figs. 2 and 3), the domains with elongated cells are closer to that limit. Due to the fact that V_{MS} increases with the surface tension, the elongated cellular morphology grew closer to the [100] or [110] direction than the one with cylindrical cells.

The reason for the appearance of the grain boundary is that the surface dendrites growing along the tube walls revealed different crystal orientations. Due to competition between the surface dendrites, certain crystal orientations prevail. With high cooling temperatures, this competition was directly observed to be quite dynamic. With low cooling temperatures, a direct observation was not possible.

Fig. 4 shows the array stability limit (calculated by the analytic expression given in Ref. [15]) as a function of solidification velocity for three different compositions (——). Although no analytical expression for the

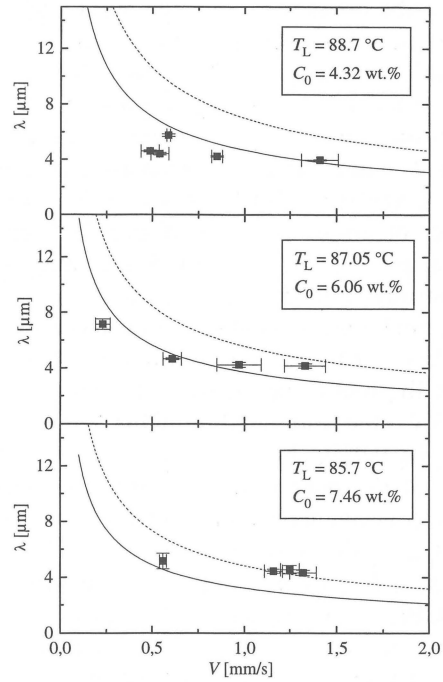

Fig. 4. Comparison of measured cell spacings with the array stability limit (——) calculated with the analytical expression given by Hunt and Lu [15] for different compositions and solidification velocities. The upper stability limit (– – –) is roughly approximated by taking 1.5 times the array stability limit.

upper stability limit is given in Ref. [15], it is roughly approximated in Fig. 4 by taking 1.5 times the array stability limit (– – –). The black dots are the experimental points from this work.

Within the velocity/concentration range covered experimentally, the calculated spacings were found to be independent of the temperature gradient G as long as the gradient is smaller than $G < 10^5$ K m^{-1}. Due to the temperatures used in the experiments and the low thermal conductivity of the transparent organic alloys, this seems to be a reasonable assumption [7].

Besides the spacings measured at low velocity and low concentration, the agreement between the experi-

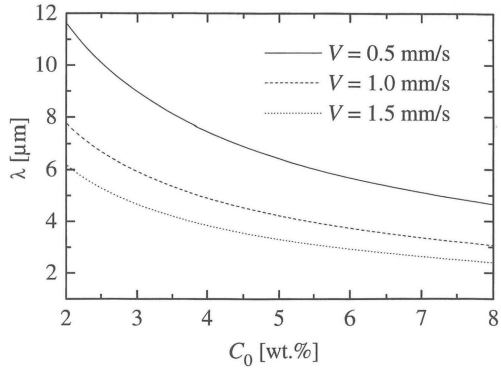

Fig. 5. The array stability limit as a function of composition for different solidification velocities calculated with the analytic expression given by Hunt and Lu [15].

ments and the prediction from the Hunt and Lu model is quite reasonable. The deviation of the low velocity/concentration points may have two different causes. First, the cellular structure needs a distance of approximately 10 times the average spacing to reach the steady state [18]. The morphologies which are evaluated in this work are taken from positions inside the tube where a solid layer of about 50 μm had already been formed. Thus spacings of larger than 5 μm may not have reached steady-state growth conditions.

The second reason might be the uncertainty in the determination of the concentration. Although the purified CBr_4 had a measured solidification interval of $\Delta T_0 = 0.3°C$, the estimated liquidus temperature was found to be 0.95°C higher than the melting temperature, T_m, of the pure CBr_4 measured by Mergy et al. [16]. It is conceivable that impurities increase T_m, but unlikely (especially if Br_2 is considered). If the impurities decrease T_m, a correction of the melting temperature of CBr_4 with respect to the value measured by Mergy et al. had to be considered and thus their measured phase diagram might be incorrect. In the literature, the following values of T_m were found: 90.1°C [20], 91.8°C [19], 92.5°C [16] and 93.4°C [21]. To investigate the influence of an uncertainty in C_0, Fig. 5 shows the array stability limit as function of the concentration for three different solidification velocities. Variations in C_0 change the spacing more markedly at low concentration and low velocities. This is consistent with the deviations of the observed spacings shown in Fig. 4(a).

4. Conclusions

The main conclusions of this work are as follows: (1) the appearance of cylindrical and elongated cellular patterns was found to be independent of concentration and velocity, within the experimental range covered; (2) cylindrical and elongated cells can either occur separately or at the same time within two (rarely three) different domains separated by a grain boundary; (3) if both morphologies are observed simultaneously, the elongated cells grew closer to the [100] or [110] direction than the cylindrical ones; (4) besides the spacings measured at low velocity and low concentration, the agreement between the experiments and the prediction from the Hunt and Lu model is quite reasonable.

Acknowledgements

The authors would like to thank A. Schillings for his assistance in various experimental details. This research was supported by the Deutsche Forschungsgemeinschaft under Sa 335/16-1, for which the authors express their gratitude.

References

[1] W. Kurz and D.J. Fisher, *Fundamentals of Solidification*, 3rd edn., Trans. Tech., Aedermannsdorf, Switzerland, 1992.
[2] D. Walton, W.A. Tiller, J.W. Rutter and W.C. Winegard, *TMS AIME, 203* (1955) 1023.
[3] W.A. Tiller and J.W. Rutter, *Can. J. Phys., 34* (1956) 96.
[4] L.R. Morris and W.C. Winegard, *J. Cryst. Growth, 5* (1969) 361.
[5] H. Jamgotchian, B. Billia and L. Capella, *J. Cryst. Growth, 64* (1983) 338.
[6] A. Ludwig and W. Kurz, *Mater. Sci. Forum, 215–216* (1996) 13.
[7] A. Ludwig and W. Kurz, *Acta Mater., 44* (1996) 3643.
[8] B. Billia and R. Trivedi, in D.T.J. Hurle (ed.), *Handbook of Crystal Growth*, Vol. 1B, Elsevier, Amsterdam, 1993, p. 899.
[9] A. Ludwig and W. Kurz, *Scr. Mater.*, accepted for publication.
[10] M.H. Burden and J.D. Hunt, *J. Cryst. Growth, 22* (1974) 109.
[11] J.D. Hunt, in *Solidification and Casting of Metals*, Metals Society, London, 1979, p. 3.
[12] W. Kurz and D.J. Fisher, *J. Cryst. Growth, 123* (1981) 11.
[13] J.D. Hunt, *Acta Metall., 39* (1991) 2117.
[14] S.-Z. Lu and J.D. Hunt, *123* (1992) 17.
[15] J.D. Hunt and S-Z. Lu, *Metall. Mater. Trans. A, 27* (1996) 611.
[16] J. Mergy, G. Faivre, C. Guthmann and R. Mellet, *J. Cryst. Growth, 134* (1993) 353.
[17] W.W. Mullins and R.F. Sekerka, *J. Appl. Phys., 35* (1964) 444.
[18] J.D. Hunt, personal communication, 1996.
[19] W.L. Kaukler and J.W. Rutter, *Mater. Sci. Eng., 65* (1984) L1.
[20] Weast (ed.), *Handbook of Chemistry and Physics*, 56th edn., Chemical Rubber Co., 1975.
[21] A.E. Korvezee, *Rec. Trav. Chim., 53* (1934) 464.